

# Physical and effective optical thickness of holographic diffraction gratings recorded in photopolymers

S. Gallego, M. Ortuño, C. Neipp, A. Márquez and A. Beléndez

Dpt. de Física, Ingeniería de Sistemas y Teoría de la Señal, Universidad de Alicante, Ap. 99, E-03080 Alicante, Spain  
[sergi.gallego@ua.es](mailto:sergi.gallego@ua.es)

I. Pascual

Departamento Interuniversitario de Óptica, Universidad de Alicante, Apartado 99, E-03080 Alicante, Spain

J. V. Kelly and J. T. Sheridan

Dept. of Electronic and Electrical Engineering, University College Dublin, Belfield, Dublin 4, Republic of Ireland

**Abstract:** In recent years the interest in thick holographic recording materials for storage applications has increased. In particular, photopolymers are interesting materials for obtaining inexpensive thick dry layers with low noise and high diffraction efficiencies. Nonetheless, as will be demonstrated in this work, the attenuation in depth of light during the recording limits dramatically the effective optical thickness of the material. This effect must be taken into account whenever thick diffraction gratings are recorded in photopolymer materials. In this work the differences between optical and physical thickness are analyzed, applying a method based on the Rigorous Coupled Wave Theory and taking into account the attenuation in depth of the refractive index profile. By doing this the maximum optical thickness that can be achieved can be calculated. When the effective thickness is known, then the real storage capacity of the material can be obtained.

©2005 Optical Society of America

OCIS codes: (090.0090) Holography, (090.2900) Holographic recording materials, (090.7330) Volume holographic gratings.

---

## References and links

1. H. J. Coufal, D. Psaltis and G. T. Sincerbox (Eds.), *Holographic Data Storage* (Springer-Verlag, New York, 2000).
2. J. E. Boyd, T. J. Trentler, K.W. Rajeev, Y. I. Vega-Cantu and V.L. Colvin, "Effect of film thickness on the performance of photopolymers as holographic recording materials," *Appl. Opt.* **39**, 2353-2358 (2000).
3. P. Cheben and M. L. Calvo "A photopolymerizable glass with diffraction efficiency near 100% for holographic storage," *Appl. Phys. Lett.* **78**, 1490-1492 (2001).
4. M. Ortuño, S. Gallego, C. García, C. Neipp, A. Beléndez and I. Pascual, "Optimization of a 1 mm thick PVA/acrylamide recording material to obtain holographic memories: method of preparation and holographic properties," *Appl. Phys. B* **76**, 851-857 (2003).
5. M. Ortuño, S. Gallego, C. García, C. Neipp and I. Pascual, "Holographic characteristics of a 1 mm thick photopolymer to be used in holographic memories," *Appl. Opt.* **42**, 7008-7012 (2003).
6. C. Neipp, J. T. Sheridan, S. Gallego, M. Ortuño, I. Pascual and A. Beléndez, "Effect of a depth attenuated refractive index profile in the angular responses of the efficiency of higher orders in volume gratings recorded in a PVA/Acrylamide photopolymer," *Opt. Comm.* **233**, 311-322 (2004).
7. M. G. Moharam and T.K. Gaylord, "Rigorous coupled-wave analysis of planar-grating diffraction," *J. Opt. Soc. Am.* **71**, 811-818 (1981).
8. M. G. Moharam and T.K. Gaylord, "Rigorous coupled-wave analysis of gratings diffraction-TE mode polarization and losses," *J. Opt. Soc. Am.* **73** 451-455 (1983).
9. M. G. Moharam and T. K. Gaylord, "Three-dimensional vector coupled-wave analysis of planar-grating diffraction," *J. Opt. Soc. Am.* **73**, 1105-1112 (1983).

10. M. G. Moharam, E. B. Grann, D. A. Pommet and T. K. Gaylord, "Formulation for stable and efficient implementation of the rigorous coupled-wave analysis of binary gratings," *J. Opt. Soc. Am A* **12**, 1068-1076 (1995).
  11. S. Gallego, M. Ortuño, C. Neipp, C. García, A. Beléndez and I. Pascual, "Overmodulation effects in volume holograms recorded on photopolymers," *Opt. Commun.* **215**, 263-269 (2003).
- 

## 1. Introduction

The technology of holographic information storage has great possibilities: with both a maximum theoretical storage 1000 times greater than that of a CDROM and a random access time of only 10% of the later [1]. In the recent years many papers have been published in this area [2-5]. Photopolymers are one of the most interesting materials to obtain holographic memories. They have an acceptable energetic sensitivity, a variable spectral sensitivity depending on the sensitizer dye used, good resolution, high diffraction efficiency and good signal/noise ratio. Their low price, easy preparation and the fact that complicated developing processes are not necessary make them even more attractive for use on a large scale in read only WORM (write once read many) type memories.

One of the basic requirements for holographic memories to be competitive is that the recording material layer must be 500  $\mu\text{m}$  or thicker [1]. A bigger number of holograms may be recorded with thicker layers, since in this case the angular Bragg selectivity is larger due to the fact that the width of the angular response curve is very small [3]. It is not easy to find such large thickness using many of the recording materials currently available. However there are easy methods of preparation to achieve thick dry layers using photopolymers as holographic recording materials [4]. Unfortunately this large physical thickness of the material does not necessarily lead to the desired decrease in the width of the angular scan: as we will see we should distinguish between the physical thickness and the effective optical recording thickness, the latter being the significant value for holographic data storage.

In photopolymers, in the recording step light is exponentially attenuated in depth inside the material, as described by Beer's law. This attenuation produces a non-uniform refractive index profile in these materials. The effect of a depth attenuated index profile in the angular response for the different orders that propagate inside the material, was examined theoretically and experimentally demonstrated by Neipp et al. [6], using a method based on the Rigorous Coupled-Wave Method (RCWA) proposed by Moharam and Gaylord [7-10]. An immediate consequence of this attenuation of the refractive index profile is a limit on the effective thickness of the material. This effective thickness does not depend of the physical thickness but on the chemical composition of the material. In this work this limitation on the effective thickness is analyzed, and the existence of a maximum optical thickness for each photopolymer composition will be demonstrated using the algorithm proposed by Neipp et al. [6].

In this work the experimental study is carried out using photopolymers based on acrylamide (AA) monomers. Thick layers are obtained using lower concentrations of dye and monomer than for standard layers (around 100  $\mu\text{m}$ ). These changes in the material composition are done to obtain higher stability and lower noise [1], although as will be demonstrated significant attenuation of the index profile is produced.

## 2. Theoretical background

Typically when apply the RCWA, the dielectric permittivity is only assumed to vary along the  $x$  and  $z$  directions, so as to study a planar diffraction grating. The study frequently is also restricted to the case of unslanted gratings, thus the dependence of the dielectric permittivity with  $x$  and  $z$  coordinates is assumed to be in the form:

$$\epsilon(x, z) = \sum_h \epsilon_h(z) \exp[jhKx] \quad (1)$$

$K$  is the modulus of the grating vector, which is related to the period of the interference fringes,  $\Lambda$ , as follows:

$$K = 2\pi/\Lambda \quad (2)$$

In the algorithm proposed [6], to include the effect of an attenuated grating profile recorded in the photopolymer material, each Fourier component of the permittivity is expressed as a function of  $z$  as:

$$\varepsilon_h(z) = \varepsilon_{h,0} \exp[-\alpha z] \quad (3)$$

where  $\varepsilon_{h,0}$  are the initial values (at  $z=0$ ) of the harmonic components of the dielectric permittivity.

To apply the RCWC we divide the diffraction grating in to  $G$  different sub-gratings each of thickness  $d_g$ . The total thickness of the hologram,  $d$ , is the sum of the thickness of the different sub-gratings.

$$d = \sum_{g=1}^G d_g \quad (4)$$

Above each sub-grating is assumed to have a periodic dielectric permittivity of the form:

$$\varepsilon_g(x) = \sum_h \varepsilon_{g,h} \exp[jhKx] \quad (5)$$

where  $\varepsilon_{g,h}$  is the  $h$ th Fourier component of the permittivity for the grating region  $g$ , which can be expressed as:

$$\varepsilon_{g,h} = \varepsilon_{0,h} \exp[-\alpha \sum_{g'=1}^g d_{g'}] \quad (6)$$

Then we apply the RCWA method [8] in each grating and in at every boundary [7]. In this work a value of  $G = 30$  is used, however the results does not change for  $G = 20$  or  $G = 40$ .

To obtain the attenuated refractive index profile we first obtain the refractive index modulation assuming the grating does not have any attenuation,  $n_{1eff}$ :

$$n_{1eff} = \arcsin\left\{[\eta_e / (\eta_e + t_e)]^{1/2}\right\} \frac{\lambda \cos \theta'}{\pi d} \quad (7)$$

where  $\eta_e$  and  $t_e$  are the experimentally measured efficiencies of the first and second orders, respectively, and  $\theta'$  is the replied angle inside the material. The value of  $\eta_e$  is normalized by the sum ( $\eta_e + t_e$ ) to correct for losses during reconstruction.

The first harmonic of the refractive index obtained by this way can be considered as an average over the entire thickness as:

$$n_{1eff} = \frac{1}{d} \int_0^d n_{1,0} \exp(-\alpha z) dz \quad (8)$$

thus

$$n_{1,0} = n_{1,eff} \frac{\alpha d}{1 - \exp(-\alpha d)} \quad (9)$$

Eventually it is easy to obtain the value of  $n_{1,0}$  related to the values of  $\alpha$  and the effective first harmonic of the refractive index,  $n_{1,eff}$ . An accurate description of this algorithm, which describes the electromagnetic field inside of the grating with attenuated index profile, can be found in reference [6].

### 3. Experimental setup

A solution of PVA (polyvinyl alcohol) in water forms the matrix and this is used to prepare the mixture of AA, BMA (N,N'-methylene-bis-acrylamide) and photopolymerization initiator system composed of TEA (triethanolamine) and YE (yellowish eosin). The PVA is supplied by Fluka, AA and TEA by Sigma, and YE by Panreac. The mixture is done under red light (concentrations of components for the different layers are in Table 1) and after evaporation of part of the water, a solid plastic film is formed on a glass plate, which constitutes the holographic recording material [4,11].

Table 1. Concentration and components of the different layer compositions

Composition	Type 1 40-220 $\mu\text{m}$	Type 2 250 $\mu\text{m}$	Type 3 750 $\mu\text{m}$	Type 4 1000 $\mu\text{m}$
AA (M)	0.44	0.45	0.31	0.31
BMA (M)	0.05	NONE	0.04	0.02
TEA (M)	0.20	0.20	0.14	0.14
YE (M)	$2.44 \times 10^{-4}$	$2.44 \times 10^{-4}$	$9.0 \times 10^{-5}$	$9.0 \times 10^{-5}$
PVA (W/V)	6-8%	16,88%	13,30%	13,30%

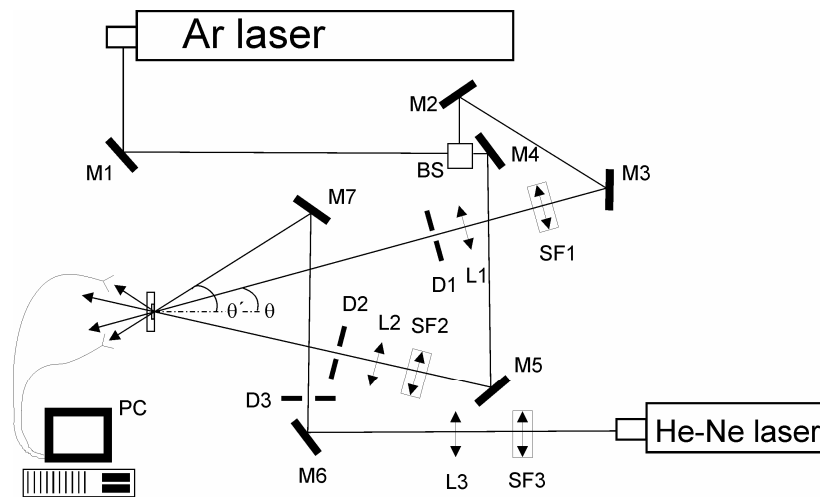


Fig. 1. Experimental setup. Where  $M_i$  are the mirrors.  $L_i$  are the lenses.  $SF_i$  the spatial filters to expand the beams.  $D_i$  represent the diaphragms. BS is the beam splitter.

To study the behavior of the photopolymeric layers, we record unslanted diffraction gratings using a holographic setup (Fig. 1). An Argon laser at a wavelength of 514 nm is used to store diffraction gratings by means of continuous laser exposure. The laser beam is split into two secondary beams with an intensity ratio of 1:1. The diameters of these beams are increased to 1.5 cm with an expander, while spatial filtering is ensured. The object and

reference beams are recombined at the sample at an angle of  $16.8^\circ$  to the normal with an appropriate set of mirrors, and the spatial frequency obtained is 1125 lines/mm. The working intensity at 514 nm is  $5 \text{ mW/cm}^2$ . The diffracted and transmitted intensity are monitored in real time with a He-Ne laser positioned at Bragg's angle ( $20.8^\circ$ ) tuned to 633 nm, where the material is not sensitive. We placed the plates on a rotating stage to measure the transmission and the diffraction efficiencies as a function of the reconstruction angle. The transmission and the diffraction efficiencies (TE and DE respectively) are calculated as the ratio of the transmitted and diffracted power, respectively, to the incident power.

#### 4. Results and discussion

The problem of the maximum limit on the optical thickness imposed by an attenuated index profile can be seen in Fig. 2 and 3. In Fig. 2 the corresponding angular scans for the diffraction efficiency are represented for two gratings stored in two photopolymer layers with the same composition (Type 1) but with a different thickness. The first curve (triangles) is obtained for a layer of  $180 \mu\text{m}$  thick and the second curve (circles) corresponds to a layer  $220 \mu\text{m}$  thick. As can be seen there are no differences in their angular widths. This occurs because their optical thickness are the same, i.e. the two diffraction gratings recorded have the same effective thickness. In Fig. 3 a similar experimental study is presented, now for layers with a different compositions (Type 1, Type 2, Type 3 and Type 4). The narrowing of the principal lobe can be observed as the physical thickness grows. Nonetheless for gratings of  $750 \mu\text{m}$  and  $1000 \mu\text{m}$  there is almost no difference in the width of the angular response, since the effective thickness of the latter is limited by the attenuation in depth of the refractive index profile.

The typical values of the index profile attenuation coefficient for a photopolymer material made of a composition of Type 1 are between  $0.010 \mu\text{m}^{-1}$  and  $0.020 \mu\text{m}^{-1}$  [6]. In Fig. 4 we simulate the angular response of the diffraction efficiency for different physical thickness using a value of  $\alpha=0.015 \mu\text{m}^{-1}$ . This figure represents the diffraction efficiency around the first Bragg's angle replay ( $20.8$ ). It can be seen that the secondary lobes have vanished and the principal lobe width stays constant for a thickness higher than  $200 \mu\text{m}$ : the optical thickness of the gratings can be considered to be  $200 \mu\text{m}$  in this case.

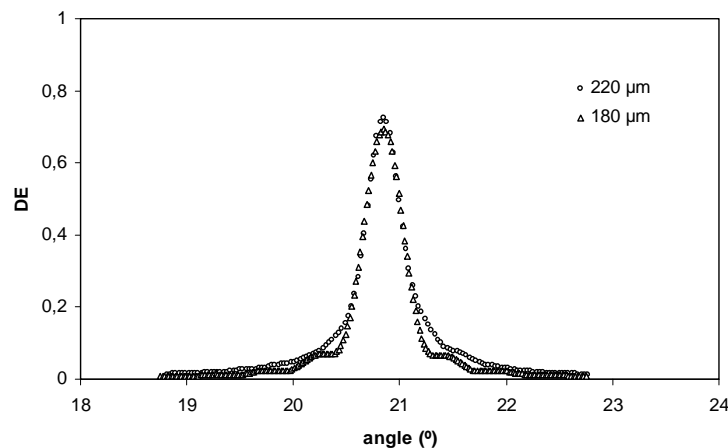


Fig. 2. Photopolymer Type 1. The experimental angular scan around the first Bragg angle ( $20.8^\circ$ ) is plotted for two layers with different physical thickness  $220 \mu\text{m}$  (circles) and  $180 \mu\text{m}$  (triangles).

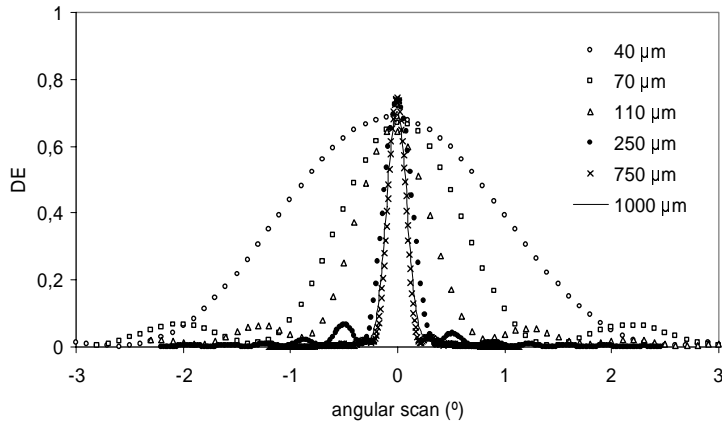


Fig. 3. The experimental angular scan around the first Bragg angle is plotted for six layers with different physical thicknesses: 40  $\mu\text{m}$  (composition Type 1), 70  $\mu\text{m}$  (composition Type 1), 110  $\mu\text{m}$  (composition Type 1), 250  $\mu\text{m}$  (composition Type 2), 750  $\mu\text{m}$  (composition Type 3) and 1000  $\mu\text{m}$  (composition Type 4).

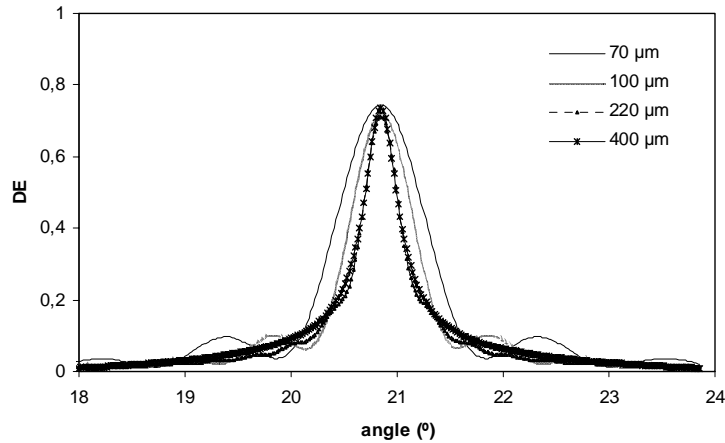


Fig. 4. The theoretical angular scan around the first Bragg angle ( $20.8^\circ$ ) is simulated using the depth attenuated algorithm for different physical thickness (70  $\mu\text{m}$ , 100  $\mu\text{m}$ , 220  $\mu\text{m}$  and 400  $\mu\text{m}$ ).

In Fig. 5 we represent the index modulation, normalized by the index modulation at the surface ( $z = 0$ ), as a function of the depth for a value of  $\alpha = 0.015 \mu\text{m}^{-1}$ . As can be seen for 200  $\mu\text{m}$  only less than 5 % of the initial index modulation is stored. For this reason, for this chemical composition, which has a specific attenuation coefficient, the optical thickness can not be higher in spite of an augment of the physical thickness of the layer.

Now, to obtain holography memories we use the chemical composition of type 3, whose  $\alpha$  coefficient ranges from  $0.005 \mu\text{m}^{-1}$  to  $0.003 \mu\text{m}^{-1}$  [6]. The decay of the normalized modulation index in depth for a value of  $\alpha = 0.003 \mu\text{m}^{-1}$  can be seen in Fig. 6. In this figure it is noticeable that the optical thickness of the grating is stopped around 1000  $\mu\text{m}$ . This effect can be seen in Fig. 7, where the diffraction efficiency around the first Bragg's angle replay ( $20.8$ ) for different thickness is represented. As it is observed the secondary lobes vanish and the width of the principal lobe is constant for thickness higher than 1000  $\mu\text{m}$ . This value can

be considered as the optical thickness of the gratings recorded with an attenuation coefficient of  $0.003 \mu\text{m}^{-1}$ .

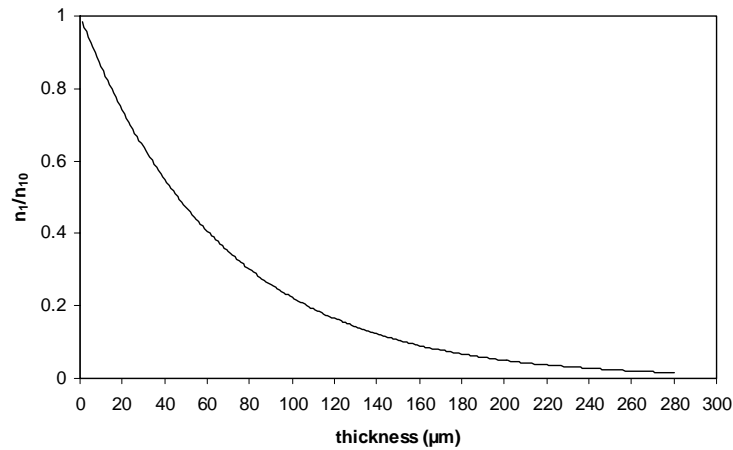


Fig. 5. The exponential decay of  $n_1$ , modulation of the refractive index, divided by the index modulation in the surface ( $n_{10}$ ) as function of depth is plotted for thin layers ( $\alpha = 0.015 \mu\text{m}^{-1}$ ).

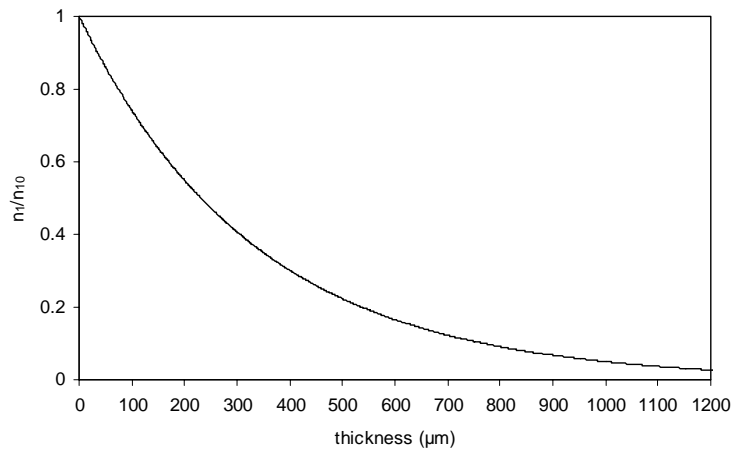


Fig. 6. The exponential decay of  $n_1$ , modulation of the refractive index, divided by the index modulation in the surface ( $n_{10}$ ) as function of depth is plotted for thick layers ( $\alpha = 0.003 \mu\text{m}^{-1}$ ).

In the ideal case, when  $\alpha = 0$ , the results predicted by the RCWA for the optical and the physical thickness are equal. In Fig. 8 the simulations when the algorithm RCWA is applied for this case are shown. In this figure the physical thickness controls the width of the central lobe. On the other hand if the curves of 600  $\mu\text{m}$  and 800  $\mu\text{m}$  of Fig. 8 are compared with the curves of the same thickness of Fig. 7, it can be observed that the curves without attenuation (Fig. 8) are narrower than the one with attenuation (Fig. 7). This effect is very important for storage applications, since it reduces the capacity of the future holographic memories recorded on photopolymers.

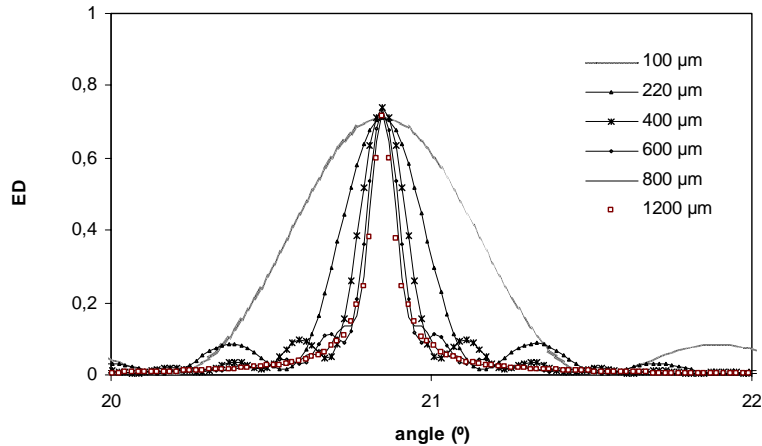


Fig. 7. The theoretical angular scans around the first Bragg angle ( $20.8^\circ$ ) is simulated using depth attenuated algorithm for different physical thickness ( $100\ \mu\text{m}$ ,  $220\ \mu\text{m}$ ,  $400\ \mu\text{m}$ ,  $600\ \mu\text{m}$ ,  $800\ \mu\text{m}$  and  $1200\ \mu\text{m}$ ).

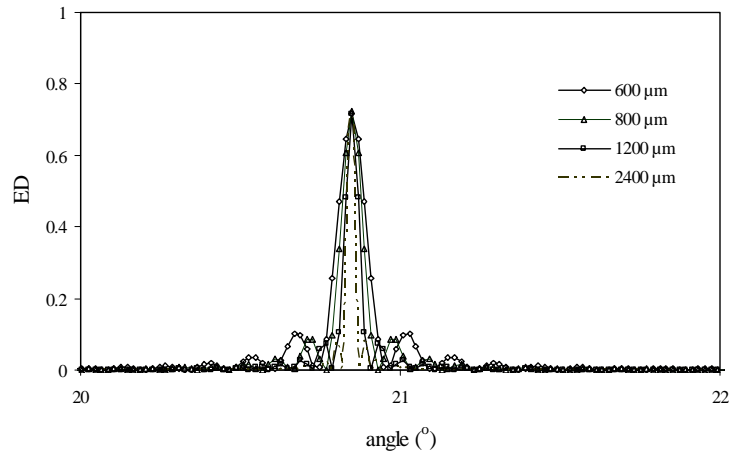


Fig. 8. The theoretical angular scans around the first Bragg angle ( $20.8^\circ$ ) is simulated using depth attenuated algorithm for different physical thickness ( $600\ \mu\text{m}$ ,  $800\ \mu\text{m}$ ,  $1200\ \mu\text{m}$  and  $2400\ \mu\text{m}$ ).

## 5. Conclusions

To achieve competitive holographic memories using photopolymers, the differences between the physical and optical effective thickness has been studied. The importance of the attenuated in depth index profile and the chemical composition in the limitation of the optical thickness of diffraction gratings recorded on photopolymers has been demonstrated, finding also good agreement between theory and experimental work. Once the composition of the material is known and using the algorithm proposed, the attenuation coefficient of the material can be found and so the maximum effective optical thickness can be found too.

Finally, the increase in of the central lobe width when a depth attenuated refractive index profile exists has been shown. This is an important problem in the research on high capacity holographic memories, if very narrow angular responses are intended to be recorded on these



materials. Using low dye and monomer concentrations a diminution of the attenuation coefficient has been observed, but an important diminution in the energy sensitivity and in the maximum diffraction efficiency is also found [4]. Therefore, in order to achieve competitive holographic memories using photopolymers as holographic recording materials, it is very important to optimize the chemical composition of the photopolymer so as to obtain a high capacity storage, while retaining acceptable energy sensitivities and high diffraction efficiencies.

### **Acknowledgments**

This work was supported by the “Oficina de Ciencia y Tecnología” (Generalitat Valenciana, Spain) under projects GV01-130 GV04A/574 and GV04A/565 and by Enterprise Ireland through Research Innovation Found and Science Foundation Ireland through the Basic Research Program.